Sieber, J., & Krauskopf, B. (2006). Tracking nonlinear oscillations with time-delayed feedback.

Tracking nonlinear oscillations with time-delayed feedback

J. Sieber[1] and B. Krauskopf[1*]

April 10, 2006

We demonstrate a method for tracking the onset of nonlinear oscillations (Hopf bifurcation) in nonlinear dynamical systems. Our method does not require a mathematical model of the dynamical system but instead relies on feedback controllability. This makes the approach potentially applicable in an experiment. The main advantage of our method is that it allows one to vary parameters directly along the stability boundary. In other words, there is no need to observe the transient oscillations of the dynamical system for a long time to determine their decay or growth. Moreover, the procedure automatically tracks the change of the critical frequency along the boundary and is able to continue the Hopf bifurcation curve into parameter regions where other modes are unstable. We illustrate the basic ideas with a numerical realization of the classical autonomous dry friction oscillator.

Notice This is the preprint version of a a conference contribution by the authors. Please cite as

J. Sieber, B. Krauskopf: *Tracking nonlinear oscillations with time-delayed feedback*. 6th International Conference on Modern Practice in Stress and Vibration Analysis, Bath (United Kingdom), 2006.

Contents

* [1]Bristol Centre for Applied Nonlinear Mathematics, Department of Engineering Mathematics, Queen's Building, University of Bristol, BS8 1TR, U.K.

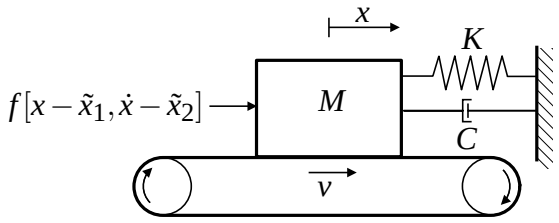

Figure 1: Set-up of an idealized dry friction oscillator with feedback f

1 Introduction

Dynamical systems can change their behavior qualitatively when one changes one or more parameters of the system. A common and typical change is a loss of stability of a stable equilibrium of the system in a Hopf bifurcation when a complex conjugate pair of eigenvalues of its linearization crosses the imaginary axis under variation of a single parameter. At the critical parameter value a family of oscillations is born. If the system is nonlinear then the oscillations are nonlinear as well, and, typically, they are either stable (*supercritical* Hopf bifurcation) or unstable (*subcritical* Hopf bifurcation). This scenario is well understood theoretically [1]. If the dynamical system is described mathematically in the form of a differential equation there are numerical tools available [1, 2] that can track curves where Hopf bifurcations occur in two-dimensional parameter planes, thus, identifying parameter regions of linear stability and regions of oscillations.

If the dynamical system is given in the form of an experiment the task of tracking the Hopf stability boundary by varying parameters is quite challenging. One approach is to run the experiment close to its stability boundary for a sufficiently long time to determine if the transients decay or grow. As the transient decay or growth is often very slow close to the stability boundary this procedure is time-consuming and produces results of low accuracy.

In this paper we present an alternative method. It assumes that the dynamical system is feedback-controllable and that the control input and the system parameters of interest can be varied automatically with a precision that corresponds to the accuracy of the desired results. The core algorithm (a *continuation*) provides an iterative computational method that prescribes a sequence of control inputs and parameter values and a criterion that decides which of these parameter values lie on the stability boundary. The computations have to be performed in parallel to running the dynamical system (for example, the experiment), but not in real time. Importantly, it is not necessary to set initial values of the dynamical system (which would involve stopping and reinitializing the experiment). Moreover, the dynamical system always remains in a stable regime with a closed stabilizing feedback loop, so that our method does not require to run the dynamical system freely close to its stability boundary.

Our method is ideally suited for dynamical systems posed by computer-controlled experiments, especially for hybrid tests such as *real-time dynamic substructuring* tests of mechanical engineering systems [3]. These tests couple an experimental test specimen of a poorly understood or critical component in real time (and bidirectionally) to a computer simulation of the remainder of the structure. One of the central goals of these hybrid experiments is the tracking of stability boundaries. The automatic and precise variation of parameters and the feedback controllability, which our method requires, are particularly easy to achieve in hybrid tests since they are in part run as a computer simulation.

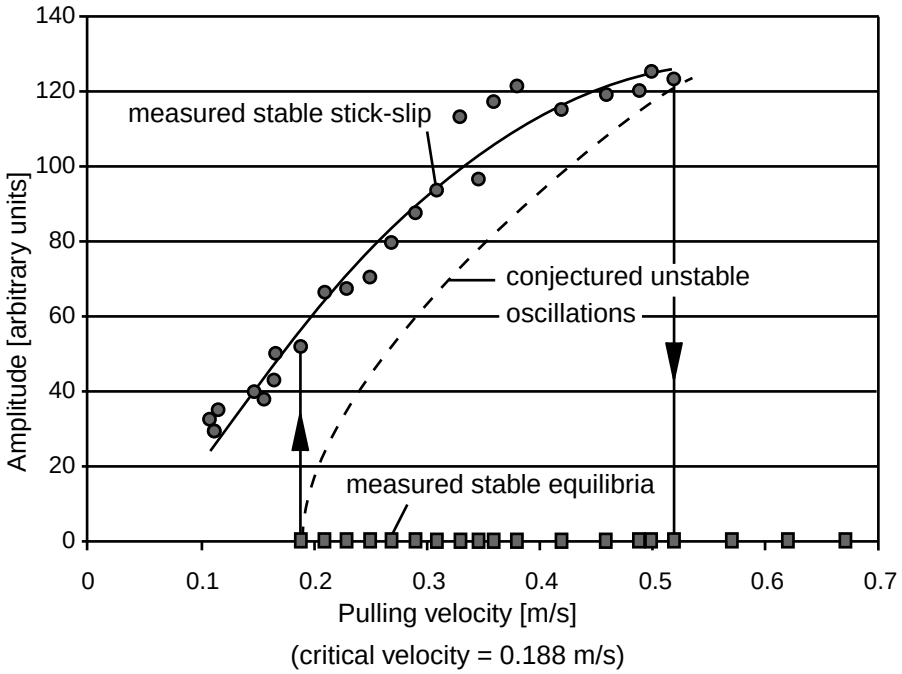

Figure 2: Diagram of the experimental results from [4] showing the velocity v versus the amplitude of oscillations. Dots show the amplitude of measured stick-slip oscillations (fitted with a solid line) and squares refer to measured equilibria. The dashed line connecting the transitions is the conjectured family of dynamically unstable periodic orbits. (Reprinted with kind permission from G. Stépán; translations from the Hungarian original courtesy of G. Orosz.)

2 The dry friction oscillator with constant forcing and feedback control

As our illustrating example we consider a dry friction oscillator with constant forcing; see Fig. 1. The friction between the running belt and the mass induces a force on the mass, pushing it against the damped spring that is fixed to the wall. The overall force on the mass at position x is $-Kx - C\dot{x} - F_f(\dot{x} - v)$ where x is measured with respect to the reference position of the relaxed spring, K is the spring constant, C is the damping, F_f is the force exerted by the friction, and v is the velocity of the running belt. The dynamic behavior of this nonlinear single-mass-spring-damper system changes qualitatively when one varies the system parameter v. For large v the rest state (equilibrium) x_0, given by $x_0 = -F_f(-v)/K$ and $\dot{x} = 0$, is stable. At a critical velocity v_h the rest state x_0 loses its stability in a subcritical Hopf bifurcation. If one decreases v gradually from above v_h to below v_h one observes a sudden transition to large-amplitude stick-slip oscillations. Similarly, when increasing v in the stick-slip oscillation regime the system jumps to a stable equilibrium at a critical velocity $v_d > v_h$. The bistability between stable stick-slip oscillations and a stable equilibrium in the parameter region $[v_h, v_d]$ has been observed experimentally in [4] for a mass on a large rotating disc; see also [5].

Figure 2 shows a sequence of experimental measurements from [4] for different values of the velocity v. Modeling and general theory predict that a family of unstable periodic orbits

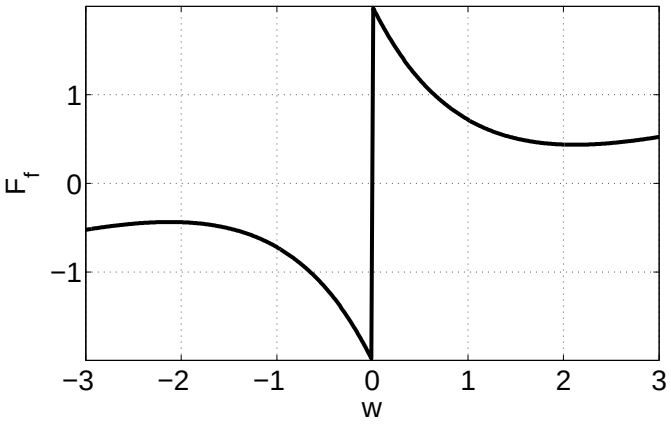

Figure 3: Friction law $F_f(w)$ used in Eq. 3 for the parameters $F_c = -0.5$, $F_s = 2$ and $F_v = 0.3$.

separates the two stable regimes for parameters v in the interval $[v_h, v_d]$.

We simulate the experiment shown in Fig. 1 under the conditions of applying an additional feedback force to the mass of the form

$$f[x - \tilde{x}_1, \dot{x} - \tilde{x}_2] = -\left(k_1[x - \tilde{x}_1] + k_2[\dot{x} - \tilde{x}_2]\right). \tag{1}$$

The output of our simulation is the time profile $(x(t), \dot{x}(t))$ of the ordinary differential equation (ODE)

$$M\ddot{x} + C\dot{x} + F_f(\dot{x} - v) + K \cdot x = -\left(k_1[x - \tilde{x}_1] + k_2[\dot{x} - \tilde{x}_2]\right) \tag{2}$$

with the dimensionless parameters $K = 1$, $M = 1$, $k_1 = 1$, $k_2 = 2$, and, initially, $C = 0$. As the friction law we choose

$$F_f(w) = [F_c + (F_s - F_c)\exp(-|w|) + F_v|w|]\,\mathrm{sign}(w), \tag{3}$$

which gives the velocity-force curve shown in Fig. 3 with the parameters $F_c = -0.5$, $F_s = 2$ and $F_v = 0.3$. In order to mimic the experimental situation we add 1% noise to the right-hand-side of Eq. 2 and to the output, and restrict the evaluation of the time profile $x(t)$ to a sampling in constant steps of length 0.01.

Eq. 2 with friction law Eq. 3 gives rise to a (subcritical) Hopf bifurcation if

$$v = -\log\left([F_v + C]/[F_s - F_c]\right).$$

Since we focus on the Hopf bifurcation and the smooth (non-sticking) unstable periodic orbits, the argument w is always negative in Eq. 3.

3 Control-based continuation of Hopf bifurcation

The procedure for control-based continuation, introduced in [6], is based on a continuation of fixed points of a nonlinear input-output map X. It can be applied as follows to the continuation of Hopf bifurcations in the context of a dry friction oscillator. Specifically, we illustrate how one can find the Hopf bifurcation curve in the (v, C)-plane.

Input-output map: The dry friction oscillator is controllable by the feedback given in Eq. 1. Thus, the dynamical system in Eq. 2 defines a map $X : \mathbb{R}^6 \mapsto \mathbb{R}^6$ in the following way. First, set the control target

$$\tilde{x}(t) = [\tilde{x}_1(t), \tilde{x}_2(t)] = \tilde{\xi} + \cos(2\pi t/T)\tilde{\eta} + \sin(2\pi t/T)\tilde{\zeta} \tag{4}$$

where $\tilde{\xi}$, $\tilde{\eta}$ and $\tilde{\zeta}$ are all in $\mathbb{R}^2$ and T is the period of the forcing. Second, let the controlled dynamical system relax to its controlled steady state $x(t)$ (which has period T). Finally, project $x(t)$ onto its first two Fourier modes:

$$\xi = \frac{1}{T}\int_0^T x(t)\,dt,\ \ \eta = \frac{2}{T}\int_0^T \cos(2\pi t/T)x(t)\,dt,\ \ \zeta = \frac{2}{T}\int_0^T \sin(2\pi t/T)x(t)\,dt. \tag{5}$$

The map X is defined by $(\tilde{\xi}, \tilde{\eta}, \tilde{\zeta}) \mapsto (\xi, \eta, \zeta)$ and depends on the parameters v and C, and the period T. One evaluation of the map X involves running the controlled dynamical system until it has relaxed. For successive evaluations of X for a sequence of $(\tilde{\xi}, \tilde{\eta}, \tilde{\zeta})$ that are close to each other it is not necessary to reset the initial values of the dynamical system.

If T is chosen appropriately and the amplitude of the forcing in Eq. 4 is small (that is, $\|\tilde{\eta}\|^2 + \|\tilde{\zeta}\|^2 - r^2 = \tilde{\eta}^T\tilde{\eta} + \tilde{\zeta}^T\tilde{\zeta} - r^2 = 0$ and r small) then the map X has a fixed point, which corresponds to an almost harmonic oscillation of amplitude r close to the Hopf bifurcation. The following continuation procedure tracks this small periodic orbit.

Initialization: Suppose we have an initial guess for a Hopf bifurcation point, its parameters (v_0, C_0), its location $\xi_0 = (x_0, 0)$, its critical frequency $1/T_0$, and its critical eigenspace $\cos(2\pi t/T_0)\eta_0 + \sin(2\pi t/T_0)\zeta_0$. We correct the initial guess by solving

$$\begin{aligned} 0 &= X(\tilde{\xi}, \tilde{\eta}, \tilde{\zeta}, T, v, C) - (\tilde{\xi}, \tilde{\eta}, \tilde{\zeta}) && (6)\\ 0 &= \tilde{\eta}^T\tilde{\eta} + \tilde{\zeta}^T\tilde{\zeta} - r^2 && (7)\\ 0 &= \zeta_{j-1}^T[\tilde{\eta} - \zeta_{j-1}] + \eta_{j-1}^T[\tilde{\zeta} - \eta_{j-1}] && (8) \end{aligned}$$

iteratively for the variable $y = (\tilde{\xi}, \tilde{\eta}, \tilde{\zeta}, T, v) \in \mathbb{R}^8$ and for fixed $C = C_0$, (small) r, and $j = 1$. The point $y_1 := (y, C_0) \in \mathbb{R}^9$ is the first point on the Hopf curve and $y_1^t = (0, 0, 0, 0, 0, 0, 0, 0, 1)$ is its initial direction.

Prediction (step j): Set $y_j^p = y_{j-1} + sy_{j-1}^t$ as initial guess for the next point on the Hopf curve. The quantity s is the pseudo-arclength step-size along the Hopf curve [1].

Correction (step j): Solve system Eq. 6–Eq. 8 extended by

$$0 = [y_{j-1}^t]^T[y - y_j^p], \tag{9}$$

iteratively starting from y_j^p. The root $y_j := (\tilde{\xi}, \tilde{\eta}, \tilde{\zeta}, T, v, C) \in \mathbb{R}^9$ is the next point on the curve and $y_j^t := [y_j - y_{j-1}]/\|y_j - y_{j-1}\|$ is the secant for the prediction step $j + 1$.

Iteration of prediction and correction is a standard procedure for the continuation of solutions of parameter-dependent nonlinear problems; it is implemented in numerical software such as AUTO [2] for the case that the dynamical system is given as an ordinary differential equation. Eq. 7 fixes the radius of the small periodic orbit, Eq. 8 fixes its phase, and Eq. 9 reparametrizes the solution curve with respect to its pseudo-arclength. Eq. 8 and Eq. 9 are well established in the context of numerical continuation methods [1]. Possible methods for the corrector iteration and the initialization are:

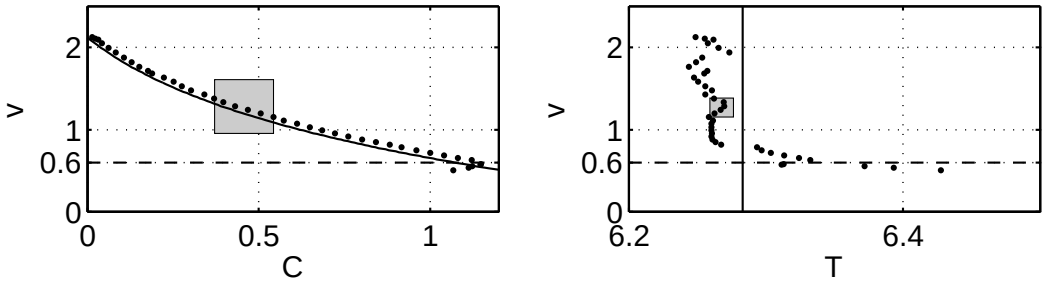

Figure 4: Result of the Hopf bifurcation continuation in the (C, v)- and (T, v)-parameter planes. The analytically known Hopf curve of Eq. 2 is shown as a solid curve. The parameter components of the solution y_j of iteration Eq. 6–9 are marked as dots. The doashed line at $v = 0.6$ marks the parameter value for the grazing event of the small periodic orbit.

(a) a relaxed fixed point iteration,
(b) a Newton iteration where the linearization of X is obtained by a finite difference approximation,
(c) a Quasi-Newton iteration (based, for example, on Broyden updates).

Stabilization by extended time-delayed feedback control [7] corresponds in its limit to the fixed point iteration (a) applied to Eq. 6. It cannot be expected to work in general, in particular, not for system Eq. 6–Eq. 9 which is close to singular for small r. The Newton iteration is expensive as it requires the evaluation of X ten times per iteration (nine times to obtain the linearization because $y \in \mathbb{R}^9$). On the other hand, it is the most robust and the available linearization can be used to compute the tangent to the curve at no extra cost. Quasi-Newton methods require only one evaluation of X per iteration, being very efficient if successful (as the cost of the linear algebra is negligible), but they are less robust.

Here we perform the continuation using a Quasi-Newton iteration for all steps $j > 1$ with a rank-one Broyden update for the linearization of Eq. 6, extended by the analytically known derivatives of Eq. 7–Eq. 9. This iteration converges quickly for system Eq. 6–Eq. 9 if one replaces X by its second iterate $X \circ X$ in Eq. 6 and chooses r not too small. The initialization step is performed with a full Newton iteration. We choose the radius $r = 0.6$, a tolerance of 0.01 for the correction (requiring at least two corrections and that the last correction step and the residual δ of system Eq. 6–Eq. 9 are below tolerance), and a maximum of 0.06 for the step-size s in the predictor.

4 Tracking the subcritical Hopf bifurcation of the dry friction oscillator

Figure 4 and Fig. 5 present the results. Figure 4 shows the solution y_j of system Eq. 6–Eq. 9 in the (C, v)-plane and in the (T, v)-plane (dots) and compares them with the analytically known Hopf curve and period (solid curve) of the underlying dynamical system Eq. 2. The procedure started at $C = 0$ and tracked the Hopf curve toward increasing C. We observe that the branch follows the Hopf curve with a small but systematic error up to $v \approx r$ ($r = 0.6$). The systematic error is caused by the finite (non-zero) amplitude of the tracked orbit and gives a

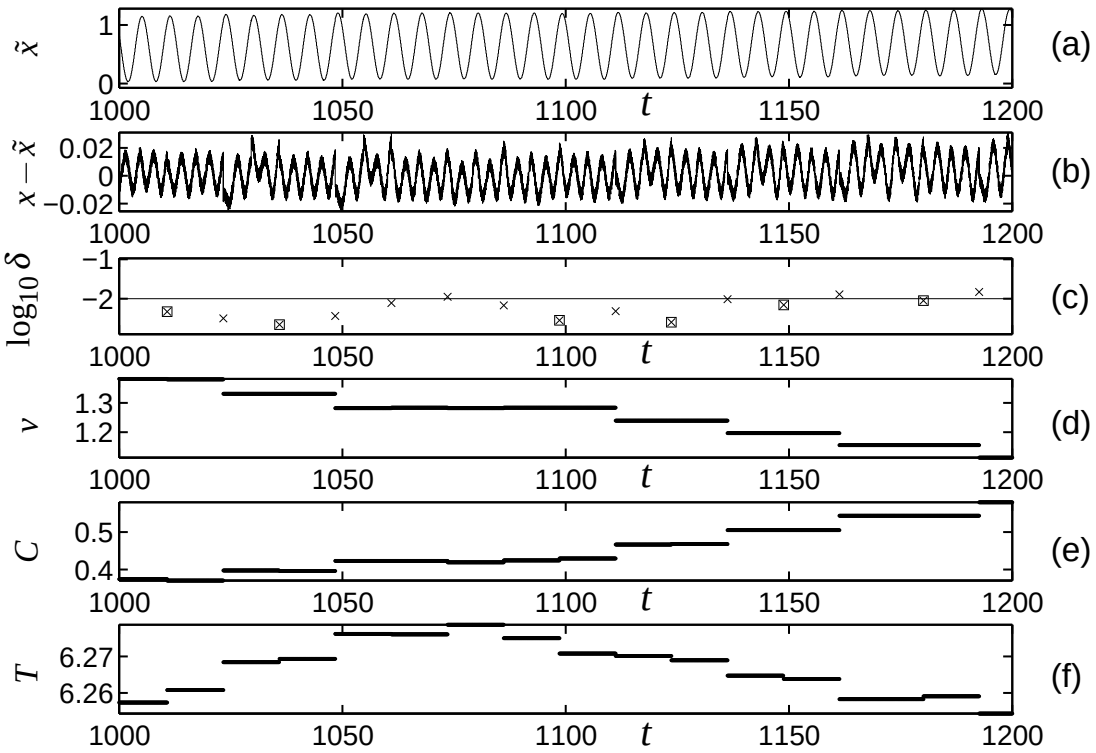

Figure 5: Time profiles along the part of the Hopf curve in the grey region of Fig. 4. Panel (a) shows the control input $\tilde{x}$, panel (b) the difference $x - \tilde{x}$ between input and output, panel (c) the logarithm of the norm of the residual δ of the right-hand-side of Eq. 6–9, and the panels (d)–(f) show the bifurcation parameters v, C and T.

deviation toward larger damping because the underlying Hopf bifurcation is subcritical (the orbit tracked by iteration of system Eq. 6–Eq. 9 is dynamically unstable).

The behavior of the solutions y_j for $v \leq r = 0.6$ shows that the method may produce spurious solutions when the the tracked small periodic orbit is no longer harmonic. At $v = r = 0.6$ (dashed line in Fig. 4) the tracked orbit grazes the discontinuity curve $\dot{x} = v$ of the friction law; see Fig. 3. This grazing gives rise to a distinctly non-harmonic stick-slip output $x(t)$. In order to be able to track the Hopf curve toward smaller v one has to decrease the radius parameter r in Eq. 7. We remark that such spurious solutions can be automatically detected in practice by comparing the output to its projection onto the first Fourier components. The correction of system Eq. 6–Eq. 9 also generates large residuals and correction steps close to the grazing event.

Figure 5 shows details of the temporal behavior of the iteration along the part of the branch in Fig. 4 that is in the grey region (around $C = 0.5$). The crosses in panel (c) show the times at which the experimental output was considered sufficiently stationary to be accepted as output of the map X. The comparison to the input $\tilde{x}$ in panel (a) shows that the relaxation toward an acceptable state takes approximately two or three periods. (The tolerance for acceptance is 10^{-3} with respect to the $\mathbb{L}^2$-norm over the period.) Figure 5(b) shows the difference between input $\tilde{x}$ and output x. The y-axis in panel (c) shows the logarithm of the Euclidean norm of the residual of the right-hand-side of system Eq. 6–Eq. 9. Figure 5(d)–(f) display the parameters v,

C and T. The squares in Fig. 5(c) mark those residuals that have been accepted as sufficiently small (together with the last correction). The parameters v, C and T at the time of acceptance correspond to dots in the grey rectangle along the curve in Fig. 4. According to Fig. 5(c), on average, the Broyden update needs less than ten evaluations of the right-hand-side of Eq. 6–9 to achieve the tolerance, making it more efficient than a full Newton iteration. Along the branch of Fig. 4 up to $v = r = 0.6$ the input-output map X has been evaluated 135 times, corresponding to an overall simulation time of 2207.24 in dimensionless units (roughly 350 periods). This excludes the initial Newton iteration, which needs 80 evaluations of X.

5 Conclusions and future work

We have presented a method that allows for direct tracking of the onset of nonlinear oscillations in nonlinear dynamical systems depending on two parameters. The method does not require a model of the dynamical system, so that it is applicable to the tracking of stability boundaries in experiments and substructuring tests.

Future work will be concerned with the implementation of this idea into prototype substructured experiments, such as mass-spring-damper and mass-spring-pendulum systems [8]. The approach outlined in this paper can also be generalized to enable it to track families of unstable nonlinear oscillations and their bifurcations (period-doubling, saddle-node, torus, symmetry-breaking and homoclinic bifurcations).

Acknowledgement

The research of J.S. is supported by EPSRC grant GR/R72020/01.

References

[1] Y.A. Kuznetsov. *Elements of Applied Bifurcation Theory*. Springer Verlag, 2004. third edition.

[2] E. J. Doedel, A. R. Champneys, T. F. Fairgrieve, Y. A. Kuznetsov, B. Sandstede, and X. Wang. *AUTO97, Continuation and bifurcation software for ordinary differential equations*, 1998.

[3] A. Blakeborough, M.S. Williams, A.P. Darby, and D.M. Williams. The development of real-time substructure testing. *Philosophical Transactions of the Royal Society of London A*, 359:1869–1891, 2001.

[4] R. Horváth. Experimental investigation of excited and self-excited vibration. Master's thesis, University of Technology and Economics, Budapest, http://www.auburn.edu/~horvaro/index2.html, 2000.

[5] G. Stépán and T. Insperger. Research on delayed dynamical systems in Budapest. *Dynamical Systems Magazine*, 2004. http://www.dynamicalsystems.org/ma/ma/display?item=85.

[6] J. Sieber and B. Krauskopf. Control-based continuation of periodic orbits with a time-delayed difference scheme. BCANM Preprint, University of Bristol, 2006. http://hdl.handle.net/1983/399.

[7] K. Pyragas. Control of chaos via an unstable delayed feedback controller. *Phys. Rev. Lett.*, 86(11):2265–2268, 2001.

[8] Y.N. Kyrychko, K.B. Blyuss, A. Gonzalez-Buelga, S.J. Hogan, and D.J. Wagg. Real-time dynamic substructuring in a coupled oscillator-pendulum system. *Proc. Roy. Soc. London A*, 462:1271–1294, 2005.